A photoactivatable Pt^{IV} anticancer complex conjugated to the RNA ligand guanidinoneomycin

Evyenia Shaili,[b] Marta Fernández-Giménez,[a] Savina Rodríguez-Astor,[a] Albert Gandioso,[a] Lluís Sandín,[a] Carlos García-Vélez,[a] Anna Massaguer,[d] Guy J. Clarkson,[b] Julie A. Woods,[c] Peter J. Sadler,*[b] and Vicente Marchán*[a]

Dedication ((optional))

Abstract: A photoactivatable Pt^{IV} complex, *trans,trans,trans*-$[Pt(N_3)_2(OH)(succ)(py)_2]$ (succ = succinylate, py = pyridine), has been conjugated to guanidinoneomycin to study the effect of this guanidinum-rich compound on the photoactivation, intracellular accumulation and phototoxicity of the pro-drug. Surprisingly, trifluoroacetic acid treatment causes the replacement of an azido ligand and the axial hydroxide ligand by trifluoroacetate, as shown by NMR, MS and X-ray crystallography. Photoactivation of the Pt-guanidinoneomycin conjugate in the presence of 5'-GMP led to the formation of *trans*-$[Pt(N_3)(py)_2(5'\text{-GMP})]^+$, as does the parent Pt^{IV} complex. Binding of the Pt^{II} photoproduct $\{PtN_3(py)_2\}^+$ to guanine nucleobases in a short single-stranded oligonucleotide was also observed. Finally, cellular uptake studies showed that guanidinoneomycin conjugation improves the intracellular accumulation of the Pt^{IV} pro-drug in two cancer cell lines, particularly in SK-MEL-28 cells. Notably, the higher phototoxicity of the conjugate in SK-MEL-28 cells than in DU-145 cells suggests a degree of selectivity towards the malignant melanoma cell line.

Introduction

Platinum-based anticancer drugs like cisplatin (**1** in Scheme 1) and its second-generation derivatives (carboplatin and oxaliplatin) are amongst the most widely used antitumour agents in chemotherapeutic regimes in the clinic.[1] However, the dose that can be administered to patients is usually limited by the appearance of severe toxic side-effects, including nephrotoxicity, neurotoxicity, ototoxicity, nausea and vomiting. Moreover, the scope of the application of these metallodrugs is frequently limited by intrinsic or acquired resistance. In this context, photoactivation can be used to improve the therapeutic efficacy of metal-based chemotherapeutics by triggering drug release from selective delivery systems or through activating a pro-drug at a desired time and place and with dosage control.[2] Taking into account that the effect of the anticancer drug will be limited to a specific irradiated area, this promising approach is expected to increase drug efficacy and reduce toxic side-effects provided that the surrounding normal tissues will not be damaged.

Photoactivatable platinum(IV) pro-drugs are attractive compounds for cancer treatment since they benefit from the advantages of classical Pt^{IV} complexes (e.g. higher stability in biological media, aqueous solubility and the possibility of oral administration),[3] and of the use of light to control the release of Pt^{II} active species by light-promoted reduction.[4] In recent years, we have developed photoactivatable *trans*-dihydroxido Pt^{IV} diazido anticancer complexes with *trans* dia(m)mine ligands.[5] These complexes are inert and nontoxic in a biological environment in the dark, but upon light irradiation, they are selectively activated and become potently cytotoxic towards a number of cancer cell lines. Replacement of one or two NH_3 ligands with pyridine in *trans,trans,trans*-$[Pt(N_3)_2(OH)_2(NH_3)_2]$ leads to higher photocytotoxicity and visible-light activation. This is an important feature for clinical applications because visible light penetrates more deeply than UVA. Indeed, *trans,trans,trans*-$[Pt(N_3)_2(OH)_2(py)_2]$ (**2** in Scheme 1A) can be activated over a range of wavelengths and is highly active against a range of cancer cell lines using low doses of visible light, including cisplatin-resistant A2780 human ovarian carcinoma cells.[6] These features together with its high stability in solution and towards gluthathione result in complex **2** being a promising lead compound for developing new photoactivatable Pt^{IV} pro-drugs.[7] The fact that these complexes platinate DNA and produce lesions that are distinctly different from those generated by cisplatin offers a potential for new mechanisms of action and non-cross-resistance with existing therapies.[8]

In recent years, the approach of using UV and/or visible light to activate anticancer metal-based pro-drugs has been extended to other metals,[9] including Ru, Re, Rh and Ir. Representative examples are ruthenium(II) arene complexes ($[(\eta^6\text{-}p\text{-cym})Ru(bpm)(py)]^{2+}$) and Ru^{II} polypyridyl complexes in which the active species are photo-released by dissociation of Ru-pyridine or Ru-thioether bonds. Very recently, ruthenium(II)[10] and rhenium(I)[11] complexes have been masked with caging groups to control their activation by UV irradiation.

In view of the potential of photoactivatable metallodrugs for cancer treatment, it is desirable to optimise their pharmacological properties (e.g. aqueous solubility and cell uptake). Moreover, the application of the so-called targeted strategies to these complexes has enormous potential for developing innovative highly-selective metal-based anticancer drugs.[12] In this context, we demonstrated the feasibility of

[a] M. Fernández-Giménez, S. Rodríguez-Astor, A. Gandioso, L. Sandín, C. García-Vélez, Dr. V. Marchán
Departament de Química Orgànica and IBUB
Universitat de Barcelona
Martí i Franquès 1-11, E-08028, Barcelona, Spain
E-mail: vmarchan@ub.edu
[b] Dr. E. Shaili, G. J. Clarkson, Prof. P. J. Sadler
Department of Chemistry
University of Warwick
Warwick, CV4 7AL, Coventry, UK
E-mail: P.J.Sadler@warwick.ac.uk
[c] Dr. J. A. Woods
Photobiology Unit, Department of Dermatology
Ninewells Hospital
Dundee, DD1 9SY, UK
[d] Dr. A. Massaguer
Departament de Biologia
Universitat de Girona
Campus Montilivi, E-17071, Girona, Spain

Supporting information for this article is given via a link at the end of the document.((Please delete this text if not appropriate))

conjugating photoactivatable Ru^{II} arene complexes to receptor-binding peptides which could then undergo photo-induced reactions with DNA.[9b] This work provided the first example of a potential Ru-based anticancer agent with a dual mechanism of selectivity. In the case of Pt^{IV} pro-drugs, derivatization of the detachable axial positions with carrier molecules can also be used to improve their pharmacological properties, such as cellular uptake and tumour selectivity,[13] as recently found by us by conjugating classical[13e] and photoactivatable[13f] Pt^{IV} complexes to RGD-containing peptides. Upconversion nanoparticles have also been used as drug carriers of photoactivated Pt^{IV} complexes.[14] Importantly, the loss of (axial) ligands upon reduction, either light-promoted (in photoactivatable Pt^{IV} complexes)[6,7,13f,14] or by intracellular reducing agents such as gluthathione or ascorbate (in classical Pt^{IV} complexes),[13,15] can cause the concomitant loss of the carrier molecule (see Scheme 1B), which would not interfere with the ultimate mode of action of the active Pt^{II} species (e.g. DNA/RNA interaction) or the potential production of reactive species (in the case of photoactivatable Pt^{IV} complexes).[6b]

Guanidinoglycosides, which are obtained by replacing the amine functions of natural aminoglycoside antibiotics with guanidinium groups,[16] are known to be taken up more efficiently by eukaryotic cells compared to their aminoglycoside precursors.[17] This feature has been exploited in the case of guanidinoneomycin, since it is able to transport large bioactive cargos into cells in a selective proteoglycan-dependent manner.[18] Recently, we described the conjugation of a cytotoxic ruthenium(II) arene complex to neomycin and to its guanidinylated derivative.[19] Ruthenium accumulation studies confirmed that guanidinylation enhanced cellular uptake of the ruthenium complex, and more importantly, that the cytotoxic activity was very dependent on the nature of the cell line, being higher in cancer than in healthy cells. This can be attributed to differences between the expression level and/or in the composition of proteoglycan receptors on the cell membrane surface.

Based on these precedents and on the promising biological activity of *trans,trans,trans*-$[Pt(N_3)_2(OH)_2(py)_2]$, now we explore the use of guanidinoneomycin as a carrier to improve the pharmacological properties of photoactivatable Pt^{IV} complexes. Such a strategy aims to contribute to the development in the near future of new RNA-targeted photoactivatable platinum anticancer complexes by using ligands which are selective for RNA. In this work, we have conjugated *trans,trans,trans*-$[Pt(N_3)_2(OH)(succ)(py)_2]$ (succ = succinylate) to guanidinoneomycin (Scheme 1A), and studied the effect of conjugation on the photoactivation of the Pt^{IV} pro-drug in the presence of 5'-GMP as a nucleobase model, as well as in the photo-induced reactions with a synthetic oligonucleotide. The phototoxicity of the compounds towards cancer cell lines in the presence of blue light and cellular uptake by ICP-MS were also investigated.

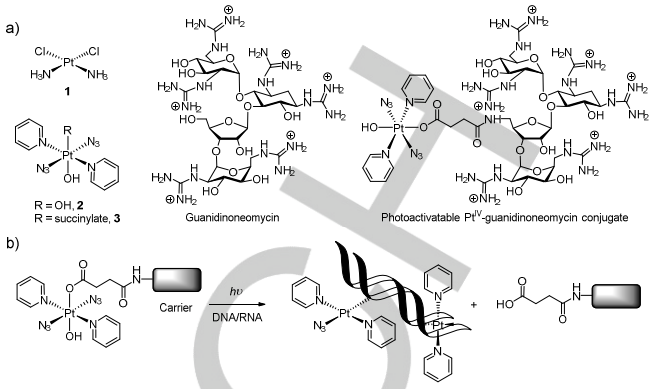

Scheme 1. a) Structure of cisplatin (**1**), *trans,trans,trans*-$[Pt(N_3)_2(OH)_2(py)_2]$ (**2**), *trans,trans,trans*-$[Pt(N_3)_2(OH)(succ)(py)_2]$ (**3**), guanidinoneomycin and of the Pt^{IV}-guanidinoneomycin conjugate. The cationic structure of guanidinoneomycin is shown since guanidinium groups are expected to be protonated under physiological conditions. b) Schematic representation of the photodissociation process and of two representative Pt^{II} adducts with a nucleic acid duplex.

Results and Discussion

Synthesis and characterization of photoactivatable Pt-guanidinoneomycin conjugates

Following previous studies on the derivatization of Pt^{IV} complexes with RGD-containing peptides,[13e,13f] we utilized *trans,trans,trans*-$[Pt(N_3)_2(OH)(succ)(py)_2]$[20] (**3**, Scheme 1) and attached it to a suitably-protected guanidinoneomycin derivative via the formation of an amide bond. Photoactivation was expected to cause the loss of the guanidinoglycoside carrier from the axial position and to generate an active Pt^{II} species (Scheme 1B).

Since the guanidinium groups, which are protonated under physiological conditions, are important for cell uptake of the compounds and for interaction with polyanionic nucleic acid targets, we conjugated complex **3** at the 5''-OH function of guanidinoneomycin.[21] This primary hydroxyl group can be regioselectively converted to an amino function. As shown in Scheme 2, the 5''-amino-5''-deoxy-Boc-protected guanidinoneomycin derivative (**6**) was prepared from the natural aminoglycoside neomycin B in a six-step synthetic route following previously reported procedures,[21] although some modifications were required for the last two steps. Firstly, after acid treatment (30% TFA in DCM) of 5''-azide-5''-deoxy-Boc-protected neomycin intermediate (**4**), guanidinylation with *N,N'*-di-Boc-*N''*-triflylguanidine afforded a complex mixture of compounds that were difficult to separate by column chromatography. However, the use of *N,N'*-di-Boc-1*H*-pyrazole-1-carboxamidine,[22] another guanidinylating reagent employed for the conversion of amino functions into *bis*-Boc-protected guanidinium groups, afforded the desired intermediate (**5**) in 64% yield after column chromatography. To our surprise, reduction of the 5''-azide group by Staudinger reaction did not afford the expected compound as reported elsewhere[21] but the iminophosphorane intermediate, which was very stable even in the presence of acidified water. Finally, reduction of the azide

function by catalytic hydrogenation afforded the expected guanidinoneomycin derivative **6** after column chromatography (40% yield).

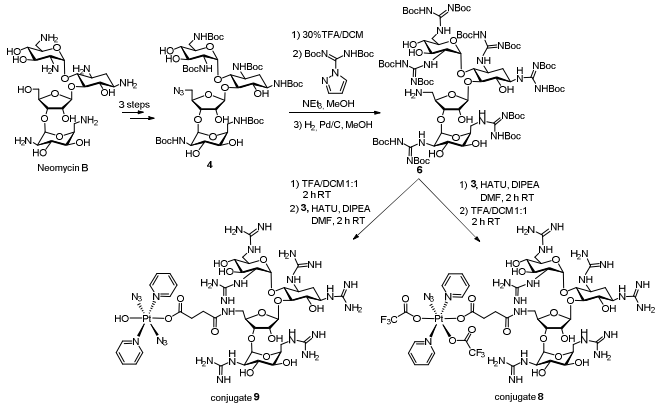

Scheme 2. Synthesis of the photoactivatable Pt^{IV}-guanidinoneomycin conjugates **8** and **9**. Although the trifluoroacetate salt of the conjugates was obtained, the neutral structures are shown.

The next step involved the covalent attachment of the Pt^{IV} complex to the guanidinoneomycin derivative. First, complex **3** was activated with HATU and DIPEA in anhydrous DMF for 2 min, and then allowed to react with **6** for 2 h at room temperature. The expected Boc-protected Pt-guanidinoneomycin conjugate (**7**) was isolated by column chromatography (yield: 89%). High-resolution ESI MS analysis afforded *m/z* values that were consistent with the calculated values of the charged species ($[M+2H]^{2+}$ and $[M+3H]^{3+}$) and with the expected isotopic distribution of platinum. Then, compound **7** was treated with a 1:1 mixture of TFA/DCM for 2 h at room temperature to deprotect the guanidinium groups. Reversed-phase HPLC analysis showed a main peak (R_t = 15.7 min; see Figure S1 in the Supporting Information) that was isolated and analyzed by HR ESI MS. To our surprise, *m/z* values ($[M+2H]^{2+}$ and $[M+3H]^{3+}$) were not consistent with the expected values for the mass of the target conjugate (**9** in Scheme 2), but instead with the formation of a modified Pt-guanidinoneomycin conjugate (**8** in Scheme 2) in which the expected hydroxido ligand in the axial position of the platinum complex as well as one of the two azido ligands (Figure 1 and Figure S2 in the Supporting Information) had been replaced by trifluoroacetate ligands. The same product was obtained when the reaction was repeated without isolating intermediate **7** by column chromatography, but by carrying out TFA deprotection at the level of the crude product. The absence of the characteristic band around 310 nm in the UV-vis spectra of conjugate **8** (Figure 1) supports the modification of the Pt moiety during the acidic treatment, particularly the loss of one azide, as evident by comparing the spectra of parent complexes **2**[6a] and **3**[20] (see the UV-vis spectra in Figure 2) and conjugate **9** (Figure 1). Conjugate **8** was fully characterized by 1D ^{1}H NMR spectroscopy and 2D COSY and TOCSY experiments. As shown in Figure 1, diagnostic signals from the platinum complex (pyridine ligands and succinate) and from guanidinoneomycin glycoside moiety (anomeric protons from the three sugars and H2 protons from the 2-deoxystreptamine ring) confirmed the covalent attachment of both moieties.

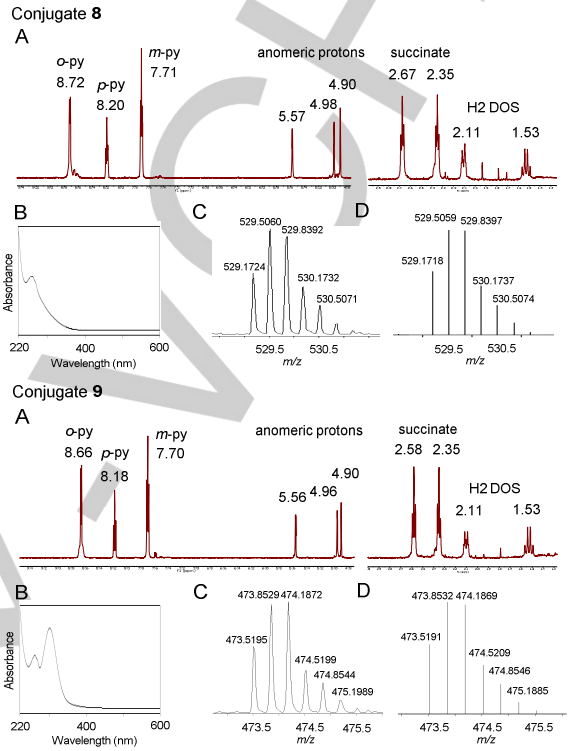

Figure 1. Characterization data for conjugates **8** (top) and **9** (bottom). (A) Expanded regions of the ^{1}H NMR spectra in D_2O and (B) UV-vis spectra of the compounds. Expanded ESI mass spectrum of the molecular peak ($[M+3H]^{3+}$), experimental (C) and calculated (D).

These unexpected results led us to evaluate the stability of photoactivatable Pt^{IV} complexes towards TFA. First, *trans,trans,trans*-$[Pt(N_3)_2(OH)_2(py)_2]$ (**2**) was allowed to react with TFA/DCM 1:1 for 2 h at room temperature. Characterization by ESI MS, NMR spectroscopy (^{1}H, ^{13}C, ^{195}Pt and ^{19}F) and X-ray crystallography revealed the formation of a new complex, *trans,trans,trans*-$[Pt(N_3)_2(CF_3COO)_2(py)_2]$ (**10**), in which both hydroxido ligands in the axial positions were replaced by trifluoroacetate (Figure 2A and Figures S11-S12). In this case, the two azido ligands were retained by the platinum center. *Trans,trans,trans*-$[Pt(N_3)_2(OH)(succ)(py)_2]$ (**3**) was also transformed into a new complex upon TFA treatment. This was characterized by MS, NMR and X-ray crystallography as *trans,trans,trans*-$[Pt(N_3)(CF_3COO)(succH)(CF_3COO)(py)_2)]$ (**11**) (succH = 3-carboxypropanoate) (Figure 2B). In this complex, the single axial hydroxido ligand was replaced by trifluoroacetate, thereby reproducing the behavior found with **2**. Interestingly, one of the two azido ligands was lost and replaced by trifluoroacetate during the acid treatment, which is in good agreement with the formation of the modified Pt-guanidinoneomycin conjugate **8**. As shown in Figure 2B, the UV-vis spectrum of complex **11** is very

similar to that of conjugate **8** (see Figure 1), and clearly different from that of the platinum complexes containing the two azido ligands (**2**, **3** and **10**). In this case, the two signals in the ^{19}F NMR spectrum of **11** (Figure S13) correspond to the two trifluoroacetate ligands (δ= -76.1 and -76.2 ppm).

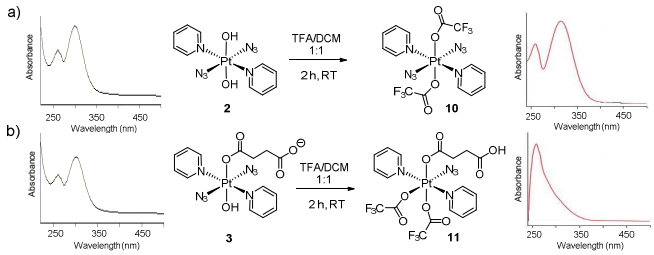

Figure 2. The contrasting reactivity of complexes **2** (a) and **3** (b) with excess TFA. The Pt^{IV} dihydroxido complex (**2**) retains both the equatorial azido ligands, whereas in the monocarboxylato complex (**3**) one azide is also replaced by trifluoroacetate. The absence of one azide is reflected in the UV-vis spectra, where the band at ca. 314 nm is lost.

Furthermore, crystals suitable for X-ray diffraction studies were obtained for both modified complexes (**10** and **11**; see Figure 3, Table 1 and Table S1 in the Supporting Information)**.** Complex **10** crystallized in the trigonal space group R-3 with 9 molecules in the unit cell whereas complex **11** crystallized in monoclinic P21/c space group with 8 molecules in the unit cell. The asymmetric unit of **11** contains two Pt^{IV} complexes, labeled A and B (Table 1), which form an H-bonded dimer via the carboxylic acid groups (see Figure S10). The bond distances between Pt^{IV} and pyridine nitrogen atoms (Pt-N1 and Pt-N2) have no significant differences between the two complexes and they fall within the range of other Pt^{IV}-diazido complexes with pyridine ligands. Similarly,[20] the Pt-N_3 bond lengths are within the expected range[23] but interestingly are significantly longer in complex **10** than in **11**, which might lead to an increased lability of the azido group. The axial Pt-O bonds (Pt-O2) from the trifluoroacetate group have no significant differences between **10** and **11A**, whereas in **11B** are longer. The Pt-O bond lengths from the succinate group resemble other Pt^{IV}-carboxylate bonds.[20] When compared to the limited examples reported for other Pt^{IV}-trifluoroacetate complexes, ranging from 1.979-2.014 Å,[24] complex **11** has longer distances (Pt-O2, O3: 2.013-2.061 Å).

The introduction of trifluoroacetate ligands into Pt^{IV} complexes has been explored by Gibson et al.[25] However in their examples, the synthesis involved reaction with trifluoroacetic anhydride, whereas herein the hydroxido ligand is replaced directly in the presence of excess of trifluoroacetic acid. Previous work has demonstrated that the pK_a of the axial hydroxide of dia(m)mine Pt^{IV}-diazido-dihydroxo complexes is ca. 3.4, suggesting that in the presence of concentrated TFA solution, the hydroxide ligand can become protonated, thus facilitating its substitution by TFA.[26] Although the trifluoroacetate ligands can confer interesting and beneficial properties (e.g. increased uptake and cytotoxicity, more facile reduction), the complexes reported in this work were found to be insoluble in aqueous media, especially complex **10**, where both axial ligands are replaced with trifluoroacetate. The replacement of one equatorial ligand with trifluoroacetate in complex **11** is an interesting outcome and the first example of a ground-state substitution of an azide in Pt^{IV}-diazido complexes, as the previously reported examples were species formed upon photosubstitution. Rationalization of the differing behaviour of parent complexes **2** and **3** is not straightforward, as the X-ray structures[20] do not show any significant difference in the lengths of Pt-N_3 bonds which might suggest a weaker bond in the ground state. The neighboring dangling terminal carboxylic acid in the case of **3** might play a role in the mechanism of substitution of the equatorial azide, for example by promoting its dissociation as N_3H, and a subsequent substitution by trifluoroacetate.

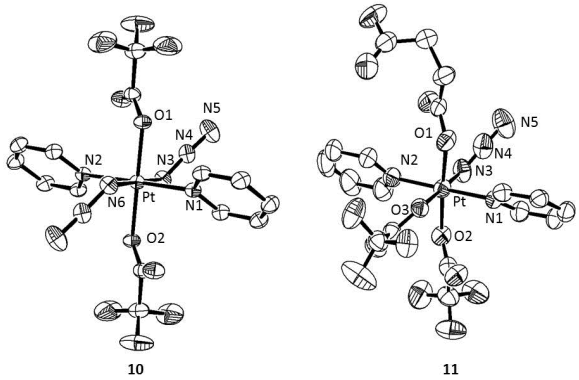

Figure 3. ORTEP diagrams for the X-ray crystal structures of **10** and **11**. The ellipsoids are set to 50% probability level. Labelling of the atoms does not represent the numbering in the cif files (CCDC 1060450-1060451) but is used to facilitate comparison between the two complexes.

Table 1. Selected bond distances and angles for complexes **10** and **11**.

Bond (Å)	Angle (°)	10	11(A)	11(B)
Pt–N1	N1–Pt–N2	2.0419(18)/ 180.0	2.033(5)/ 178.9(3)	2.027(8)/178.9(4)
Pt–N2	N3–Pt–N6 or	2.0419(18)/ 180.0	2.029(6)/ 179.3(2)	2.031(9)/170.4(8)
	N3–Pt–O3			
Pt–N3	O1–Pt–O2	2.0558(19)/180.0	2.010(7)/ 176.31(19)	2.015(3)/176.3(3)
Pt–N6	Pt–N3–N4	2.0558(19)/ 115.51(15)	NA/ 115.3(6)	NA/ 118(2)
Pt–O1	N3–N4–N5	2.0093(15)/175.6(2)	1.995(5)/ 173.6(9)	2.006(7)/168(4)
Pt–O2	-	2.0093(15)	2.012(5)	2.061(7)
Pt–O3	-	NA	2.049(5)	2.044(7)

Taking into account the unexpected reactivity of photoactivated Pt^{IV} complexes based on the parent *trans,trans,trans*-[$Pt(N_3)_2(OH)_2(py)_2$] (**2**), an inverse approach was explored for the synthesis of the Pt-guanidinoneomycin **9** (Scheme 2). The guanidinoneomycin derivative **6** was first deprotected with TFA/DCM 1:1, and the resulting trifluoroacetate salt of 5''-amino-5''-deoxy-guanidinoneomycin was allowed to react with complex **3** by using HATU as activating reagent in the presence of DIPEA. Reversed-phase HPLC analysis of the reaction crude showed

the presence of three main peaks (Figure S5) that were isolated and analyzed by HR ESI-MS. The product with lower retention time (R_t =12.0 min) was characterized by MS, ^{1}H NMR and UV-vis as the expected Pt-guanidinoneomycin conjugate (**9**), which was obtained as a white solid after purification by HPLC and lyophilization (yield: 29%). The peaks with higher retention time were characterized by MS as conjugates incorporating two Pt moieties. Despite the lower nucleophilicity of guanidinium compared with an amino function, the use of a potent amide-forming reagent accounts for this result. As shown in Figure 1, the UV-vis spectrum of conjugate **9** was similar to that of the parent Pt complexes **2**[6a] and **3**[20] (Figure 2) and HR ESI MS analysis afforded *m/z* values that were consistent with the calculated value of the charged species ($[M+2H]^{2+}$ and $[M+3H]^{3+}$) and with the expected isotopic mass distribution patterns of platinum (see Figures 1 and S6). Although the ^{1}H NMR spectrum of conjugate **9** was almost identical to that of **8** (Figure 1 and S7), chemical shifts for the protons close to the platinum center (e.g. the *ortho* protons in pyridine ligands and the methylene of the succinate) were slightly shifted to lower fields in the modified conjugate. This is in agreement with the electron-withdrawing character of the two trifluoroacetate ligands coordinated to the Pt center in conjugate **8**.

Photo-induced reactions with 5'-guanosine monophosphate. Next we studied the photoactivation of conjugate **9** to determine how the derivatization of the axial position of *trans,trans,trans*-$[Pt(N_3)_2(OH)_2(py)_2]$ with guanidinoneomycin affects its photochemical properties and the type of photoadducts formed with nucleic acids. Modified conjugate **8** was investigated to determine whether it could still be photoactivated to give Pt^{II} photoproducts despite the presence of only one azido ligand. Electron transfer from two azido ligands to Pt^{IV} can generate Pt^{II} and azidyl radicals.[6b] If only one azide is present, and this is retained in the Pt^{II} photoproduct, then the two electrons required for the reduction of Pt^{IV} need to be donated by other ligands such as the trifluoroacetate or the carboxylate. *In situ* photo-induced reactions were carried out by irradiating an aqueous solution of the conjugate (35 µM) with visible light at 310 K in the presence of 5'-guanosine monophosphate, 5'-GMP (2 mol equiv), as a simple model for nucleic acid binding and monitored by reversed-phase HPLC (see Figure S15). As shown in Figure 4, irradiation led to a decrease in the concentration of conjugate **9** and of 5'-GMP, and the appearance of a major product that was isolated and characterized by HR ESI-MS as the Pt^{II} adduct *trans*-$[Pt(N_3)(py)_2(5'\text{-GMP})]^+$ (**12**) (Figure S16). Traces of the adduct *trans*-$[Pt(py)_2(5'\text{-GMP})_2]^{2+}$ (**13**) were also detected by MS-HPLC (GMP is considered neutral in the formulae). The photorelease of the succinate-derivative of guanidinoneomycin (**14**) was confirmed by MS-HPLC since absorption of this compound in the UV region is too small to be detected. These results agree with those found previously for the parent complex (**2**)[6a] or its succinate derivative (**3**),[13f,20] and demonstrate that the covalent attachment of guanidinoneomycin does not modify the photoactivation properties of the platinum complex and the reactivity of the photoproducts for guanine nucleobase. It is interesting to note that several intermediate compounds were formed during the irradiation process (see Figure S15 in the Supporting Information) that evolved into the main adduct **12**.

To our surprise, the modified conjugate **8** was also photoactivated, but at a much faster rate. As shown in Figure 4, adduct **12** was again the major compound identified in the reaction mixture, thereby reproducing the results obtained with **9**. These results prompted us to evaluate the stability of both compounds in the dark in the presence of 5'-GMP. After incubation for 18 h at 310 K, HPLC analysis revealed that the peak for conjugate **9** was unaltered, whereas that of conjugate **8** was reduced by 25% leading to the formation of adduct **12** (Figure S17). This seems to indicate that trifluoroacetylation of the axial position together with the replacement of an azido ligand by trifluoroacetate in the platinum coordination sphere led to a complex with low stability that could be thermally activated as well.

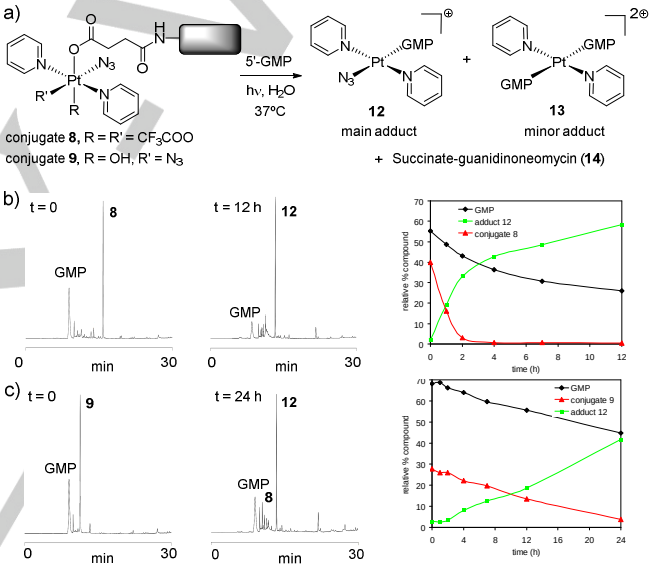

Figure 4. Photo-induced reactions of Pt^{IV}-guanidinoneomycin conjugates with 5'-GMP under visible light irradiation. A 1 M aqueous solution of $NaNO_2$ was used to filter out the UV and ensure the appropriate wavelength range (> 400 nm). (A) Schematic representation of the photoproducts, (B) reversed-phase HPLC traces for the *in situ* reaction between 5'-GMP and conjugate **8**, and (C) conjugate **9** at t= 0 and after 12 or 24 h of irradiation at 310 K, respectively, and representation of the distribution of products with time.

Photo-induced reactions with $^{5'}$dCATGGCT

Once the reactivity of Pt-guanidinoneomycin conjugates with the model 5'-GMP under visible light irradiation had been demonstrated, we investigated the ability of the most stable conjugate (**9**) to platinate a synthetic oligodeoxynucleotide sequence. We selected $^{5'}$dCATGGCT as a simple model since it contains two consecutive guanine nucleobases which are the preferred GG target sequence of cisplatin. Moreover, it has been used previously as a nucleic acid model to study the interaction with conjugates between a dicarba analogue of octreotide and a dichloridoplatinum(II) complex or a photoactivated ruthenium(II) arene complex.[9b]

First, a mixture of conjugate **9** and 5´dCATGGCT (4:1 mol ratio) was irradiated with visible light (λ > 400 nm) at 310 K for 24 h. According to previous studies with 5'-GMP (see Figure 4C), conjugate **9** was expected to be completely photoactivated within this time. Reversed-phase HPLC analysis showed the presence of three major peaks with higher retention times than the parent oligonucleotide (R_t = 24.2, 24.5 and 30.0 min; relative ratio 1:1.1:1.6, respectively; see Figure 5), which were isolated and characterized by MALDI-TOF MS (see Figure S19 in the Supporting Information). The two products with similar hydrophobicity correspond to isomeric platinated DNA adducts in which a single platinum fragment, $\{PtN_3(py)_2\}^+$, was coordinately bound to the DNA strand (**15a-b**) (Figure 5). The most hydrophobic compound was characterized as a DNA adduct incorporating two $\{PtN_3(py)_2\}^+$ fragments (**15c**). In addition, several minor compounds were identified by MS, such as oligonucleotide adducts with a single $\{Pt(py)_2\}^{2+}$ fragment (R_t = 20.8 min) or with two different platinum fragments, $\{PtN_3(py)_2\}^+$ and $\{Pt(py)_2\}^{2+}$, (R_t = 24.9 min). Enzymatic digestion with 5´- and 3´-exonucleases (bovine spleen and snake venom phosphodiesterases, respectively) in combination with MALDI-TOF MS analysis confirmed the position of the platinum fragments in the three major compounds.[27,28] As expected from the known preference of Pt^{II} complexes for nucleobases, platination occurred at the two guanines in the oligonucleotide sequence: a single $\{PtN_3(py)_2\}^+$ was bound to 3'G in **15a** or to 5'G in **15b**, whereas the two platinum moieties were bound to both guanines in **15c**.

As a control, the reaction between 5´dCATGGCT and *trans,trans,trans*-$[Pt(N_3)_2(OH)(succ)(py)_2]$ (**3**) (2 mol equiv) was also studied (Figure S20). The same major adducts were formed, as inferred by HPLC and MS, which confirms again that the photoactivation of **3** or its guanidinoneomycin conjugate **9** lead to the same Pt^{II} photoproducts that react in a similar way with the model oligonucleotide sequence. These results are in good agreement with photoreactions carried out with **9** in the presence of 5'-GMP since in that case the major photoproduct was *trans*-$[Pt(N_3)(py)_2(5'\text{-GMP})]^+$ (**12**) which retained the two pyridines and one azide as well. Although guanidinoneomycin conjugation may modify the final nucleic acid target of the photoactivated Pt^{IV} complex, the formation of similar photoadducts with complex DNA or RNA structures would be expected.

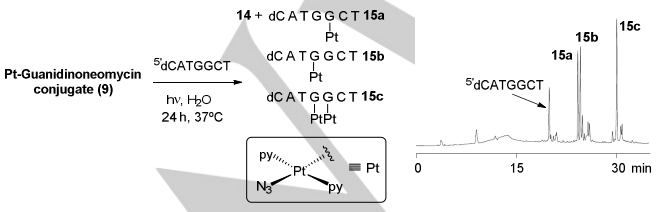

Figure 5. *In situ* photo-induced reactions of conjugate **9** with 5'dCATGGCT. A 1 M aqueous solution of $NaNO_2$ was used to filter out the UV and ensure the appropriate wavelength range (> 400 nm). Schematic representation of the photoadducts and reversed-phase HPLC traces after 24 h of irradiation at 310 K.

Cellular uptake and phototoxicity studies.

The antiproliferative potency of metallodrugs depends not only on their structures but also on cellular uptake.[29] In the case of the Pt-guanidinoneomycin conjugate, the guanidinium-rich carrier is likely to have a major influence on the cell accumulation of the photoactivated Pt^{IV} pro-drug. Highly positively-charged compounds like guanidinoglycosides might have higher uptake efficiencies than typical carriers based on poly-arginine peptides.[17,30] For this purpose, human malignant melanoma cells (SK-MEL-28) and human prostate carcinoma cells (DU-145) were exposed to 10 μM Pt-guanidinoneomycin conjugate (**9**) in the dark for 1 h. The two parent complexes, *trans,trans,trans*-$[Pt(N_3)_2(OH)_2(py)_2]$ (**2**) and *trans,trans,trans*-$[Pt(N_3)_2(OH)(succ)(py)_2]$ (**3**) were also included in the study for reference purposes. The intracellular levels of platinum were quantified by inductively-coupled plasma mass spectrometry (ICP-MS) using ^{196}Pt detection.

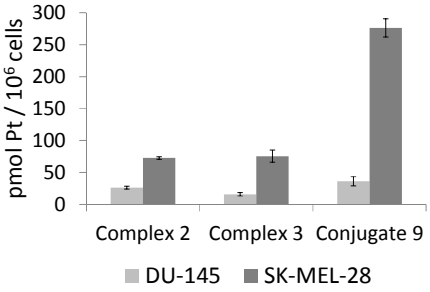

Figure 6. Cell accumulation of platinum in SK-MEL-28 and DU-145 cells after exposure to complexes **2**- **3** and conjugate **9** (10 μM, dark, 310 K, 1 h). The platinum content is related to the cell number. Errors bars represent the standard deviation of three replicates ± SD.

As shown in Figure 6, the accumulation of platinum after exposure of SK-MEL-28 cells to Pt-guanidinoneomycin conjugate (**9**) (276.2 ± 14.3 pmol Pt/10^6 cells) was about 4-fold higher than that of the two parent complexes (72.6 ± 1.9 pmol Pt/10^6 cells for **2** and 75.4 ± 9.6 pmol Pt/10^6 cells for **3**). These results confirm the beneficial effect of guanidinoneomycin conjugation on the intracellular accumulation of the Pt^{IV} pro-drug. Notably, the accumulation of conjugate **9** was considerably lower (about 8-fold) in DU-145 cells compared with SK-MEL-28 cells, which suggests a preference for the malignant melanoma cell line. Such differences in intracellular accumulation dependent on the cell type were also found with a Ru-guanidinoneomycin conjugate[19] and can be attributed to differences between SK-MEL-28 and DU-145 cells in the expression level and/or in the composition of negatively charged cell-surface proteoglycans.[18,31] Despite the reduced uptake of the three compounds in DU-145 cells compared with SK-MEL-28 cells, it is interesting to note that the accumulation of conjugate **9** (36.2 ± 7.1 pmol Pt/10^6 cells) was still higher than that of complex **2** (about 1.4-fold; 26.2 ± 2.4 pmol Pt/10^6 cells) and **3** (about 2.3-fold; 15.9 ± 2.7 pmol Pt/10^6 cells), which again

highlights the positive effect of guanidinoneomycin on the uptake of the photoactivated platinum pro-drug.

Finally, we studied the phototoxicity of the Pt-guanidinoneomycin conjugate **9** and the control complexes **2** and **3** upon irradiation with visible light (λ_{max}= 420 nm, 5 J/cm^2) in SK-MEL-28 and DU-145 cells. The photoactivated dose-dependent inhibition of cell viability is summarised in Table 2, and the cytotoxicity plots are shown in Figure S21 (see the Supporting Information). As shown in Table 2, both the conjugate **9** and the parent succinylated complex **3** showed the same phototoxicity towards SK-MEL-28 cells (IC_{50} = 15.5 μM), which was slightly lower than that of complex **2** (IC_{50} = 10.2 μM). The phototoxicity of the three compounds was reduced in DU-145 cells compared with SK-MEL-28 cells: complex **3** (IC_{50} = 20 μM) more phototoxic than **2** or **9** (IC_{50} = 43 and $\geq$ 48 μM, respectively). The higher sensitivity of SK-MEL-28 cells to this family of photoactivated Pt^{IV} pro-drugs is particularly relevant since the malignant melanoma cell line is known to be resistant to many anticancer drugs, including cisplatin.[32] Again, the fact that the phototoxic activity of the Pt^{IV} complex towards SK-MEL-28 cells was maintained upon conjugation of **3** with guanidinoneomycin but reduced in DU-145 cells, seems to suggest some selectivity for malignant melanoma cells.

Table 2. IC_{50} values of 5 J/cm^2 visible light irradiated human DU-145 and SK-MEL-28 cells pretreated with *trans,trans,trans*-[Pt(N$_3$)$_2$(OH)$_2$(py)$_2$] (**2**), *trans,trans,trans*-[Pt(N$_3$)$_2$(OH)(succ)(py)$_2$] (**3**) and the Pt-guanidinoneomycin conjugate (**9**).

Cell line	SK-MEL-28			DU-145		
Compound	IC_{50}[a] (μM) (95% CI)		Viability ± SE at [b]MAD (%)	IC_{50}[a] (μM) (95% CI)		Viability ± SE at [b]MAD (%)
2	10.2	(7.9-13.0)	74.2 ± 9.2	43.2	(33.0-56.6)	62.4 ± 13.8
3	15.5	(10.2-23.6)	130.2 ± 12.9	20.0	(14.7-27.3)	89.3 ± 4.5
9	15.5	(12.1-19.7)	99.4 ± 12.9	>48	NA	86.0 ± 4.3

[a] IC_{50} is defined as the concentration of compound that inhibits dye uptake by 50%. The lowest value indicates the highest toxicity to cells. [b] MAD: the viability of the sham-irradiated cells at the maximum administered dose.

As shown in Table 2, a higher phototoxicity was found in the melanoma cancer cells that accumulated a higher amount of each compound compared with prostate carcinoma cells. However, to our surprise, the phototoxicity of the Pt-guanidinoneomycin conjugate (**9**) towards SK-MEL-28 cells was not increased with respect the parent complexes despite the considerably higher intracellular accumulation (about 4-fold). The existence of a different mechanism of action for the parent Pt complexes and the guanidinoneomycin conjugate could account for this result. In fact, guanidinoneomycin cannot be considered a simple passive carrier that improves cellular uptake and accumulation of the platinum pro-drug, but an active molecule that could modify the final target of the photoactivated Pt^{IV} pro-drug. Hence, after internalization and accumulation inside the target cancer cells, the Pt-guanidinoneomycin conjugate could interact preferentially with RNA molecules based on the high binding affinity and selectivity of aminoglycosides and their guanidinylated derivatives for RNA compared with DNA.[33] This would facilitate RNA platination by photoreleased cytotoxic Pt^{II} species from the RNA-bound conjugate and, consequently, modify the photocytotoxic activity of the parent Pt^{IV} pro-drug.

Conclusions

In summary, we report the synthesis and characterization of a conjugate (compound **9**) between a photoactivated platinum(IV) pro-drug, *trans,trans,trans*-[Pt(N$_3$)$_2$(OH)$_2$(py)$_2$] (**2**), and guanidinoneomycin, a known RNA-binding ligand. The aim was to use this polycationic compound to promote the intracellular accumulation and targeting of a phototoxic platinum pro-drug. Photoactivatable Pt^{IV} complexes offer the possibility of a spatial and temporal control on the release of Pt^{II}-based cytotoxic species upon visible light irradiation, and the guanidinoneomycin vector can potentially promote platination of RNA over DNA, which would result in chemotherapeutic agents with a novel mechanism of action.

First, we discovered the unexpected reactivity of *trans*-diazido Pt^{IV} complexes towards trifluoroacetic acid. Low-spin 5d^6 Pt^{IV} complexes are classically inert towards ligand substitution, which has been our previous experience with these diazido complexes (in the dark).[5-7] We observed particularly the replacement of an azido ligand by trifluoroacetate and trifluoroacetylation of the free axial position in *trans,trans,trans*-[Pt(N$_3$)$_2$(OH)(succ)(py)$_2$] (**3**), as inferred by NMR, MS and X-ray crystallography. Despite the reduced stability of a Pt-guanidinoneomycin conjugate (**8**) containing this modified Pt^{IV} complex, visible light irradiation in the presence of 5'-GMP led to the formation of the adduct *trans*-[Pt(N$_3$)(py)$_2$(5'-GMP)]$^+$ (**12**), a similar pathway to that followed by the parent complexes **2** and **3**. This result opens the door to the design of new mono azido-containing photoactivatable Pt^{IV} complexes that might be used as chemotherapeutic agents. Photoactivation of the unmodified Pt-guanidinoneomycin conjugate **9** in the presence of a short single-stranded oligonucleotide led to the platination of guanine with {PtN$_3$(py)$_2$}$^+$, mirroring the result observed upon photoactivation of **9** in the presence of 5'-GMP at which adduct **12** was formed. Notably, guanidinoneomycin conjugation improved the intracellular accumulation of the Pt^{IV} pro-drug in two cancer cell lines, particularly in SK-MEL-28 melanoma cells (about 4-fold), although the phototoxic activity was similar to that of the parent complex **3**. Interestingly, the phototoxicity of conjugate **9** was reduced in DU-145 human prostate cells, which points to a degree of selectivity towards melanoma cancer cell lines.

In view of the high biological relevance of RNA as a drug target and its ability to be platinated by Pt^{II} complexes such as cisplatin and derivatives,[21,34] selective light-triggered RNA platination by photoactivatable Pt^{IV} pro-drugs could offer new opportunities to treat human diseases such as cancer. Work is in progress to

further investigate the effect of guanidinoneomycin conjugation on the biological activity of such photoactivated Pt^{IV} pro-drugs.

Experimental Section

Materials and Methods. Unless otherwise stated, common chemicals and solvents (HPLC grade or reagent grade quality) were purchased from commercial sources and used without further purification. Peptide grade DMF was from Scharlau. Milli-Q water was directly obtained from a Milli-Q system equipped with a 5000-Da ultrafiltration cartridge.

NMR spectra were recorded at 298 K on a Varian Mercury 400 MHz, Bruker AV-400 MHz or Bruker 500 MHz spectrometers, using deuterated solvents. Tetramethylsilane (TMS) was used as an internal reference (δ 0 ppm) for ^{1}H spectra recorded in $CDCl_3$ and the residual signal of the solvent (δ 77.16 ppm) for ^{13}C spectra. For CD_3OD, acetone-d_6, DMSO-d_6 or D_2O, the residual signal of the solvent was used as a reference. ^{195}Pt NMR was referenced with K_2PtCl_6 (D_2O) set to 0 ppm.

High-resolution MALDI-TOF mass spectra were recorded on a 4800 Plus MALDI-TOF/TOF spectrometer (Applied Biosystems) in the positive mode, using 2,4-dihydroxybenzoic acid as a matrix. ESI mass spectra (ESI-MS) were recorded on a Micromass ZQ instrument with single quadrupole detector coupled to an HPLC. High-resolution electrospray mass spectra (HR ESI MS) were obtained on an Agilent 1100 LC/MS-TOF or Agilent 6130 single Quad instrument.

Analytical reversed-phase HPLC analyses were carried out on a Jupiter Proteo column (250x4.6 mm, 4 µm, flow rate: 1 mL/min), using linear gradients of 0.045% TFA in H_2O (solvent A) and 0.036% TFA in ACN (solvent B). In some cases, small-scale purification was carried out using the same column. Large-scale purification was carried out on a Jupiter Proteo semipreparative column (250 x 10 mm, 10 µm, flow rate: 3 mL/min), using linear gradients of 0.1% TFA in H_2O (solvent A) and 0.1% TFA in ACN (solvent B). After several runs, pure fractions were combined and lyophilized.

Suitable single crystals of $C_{14}H_{10}F_6N_8O_4Pt$ (**10**) and $C_{18}H_{15}F_6N_5O_8Pt$ (**11**) were selected and mounted on a glass fibre with Fromblin oil and placed on an Oxford Diffraction Xcalibur Gemini diffractometer with a Ruby CCD area detector. The crystals were kept at 150(2) K during data collection. Using Olex2,[35] the structures were solved with the Superflip[36] structure solution program using Charge Flipping and refined with the ShelXL[37] refinement package using Least Squares minimisation. In the Pt1 complex of **11**, the CF_3 group was modelled as disordered by a small rotation of the CF_3 group. This refined to an occupancy of 9:1. In the Pt2 complex, both trifluoroacetate ligands were modeled as disordered over two positions related by a rotation about the bound carboxylate oxygen – carboxylate carbon bond (so each disordered molecule shares the bound oxygen of the major component). The disorder of the two trifluoroacetate ligands was linked to avoid steric clashes of the disordered components. The disorder was linked to a free variable. The occupancy of trifluoroacetates O47-F49C and O50-F52C to minor components O47-F49F and O50-F52F (as labelled in the cif files) was 54:46. The azide ligand on Pt2 complex modeled as disordered about two positions related by a small shift in the position of attachment of the azide to Pt2. The occupancy of the two components was linked to a free variable that refined to an occupancy of 59:41. All minor components were refined isotropically. The Pt2-N3 bond length as well as the Pt-N3-N4 and N3-N4-N5 angles, as depicted in Table 1 were calculated by taking the average of the two azide positions.

All the syntheses and purifications were carried out in the dark with minimal light exposure.

Synthesis and characterization of guanidinoneomycin derivatives 6 and 7.

5''-Azide-5''-deoxy-Boc-protected guanidinoneomycin derivative (5). 5''-azide-5''-deoxy-Boc-protected neomycin derivative (**4**)[21] (144 mg, 0.13 mmol) was dissolved in a 1:1 (v/v) mixture of TFA/DCM (16 mL) and allowed to react for 45 min at RT. After evaporation *in vacuo*, several co-evaporations with toluene and DCM were carried out to remove TFA completely. The white solid residue was dissolved in MeOH (4 mL) and TEA was added (1.62 mL). After addition of *N,N'*-di-Boc-1*H*-pyrazole-1-carboxamidine (331 mg, 1.07 mmol), the reaction mixture was stirred at RT for 60 h. Once the reaction reached completion (TLC and MS analysis), the solvent was removed *in vacuo*. Purification by silica gel flash-column chromatography (gradient: 0-8 % of MeOH in DCM) afforded the desired product as a white solid (175 mg, 64%). R_f (5% MeOH in DCM): 0.45; ESI MS, positive mode: *m/z* 2093.52 (calcd mass for $C_{89}H_{154}N_{21}O_{36}$ $[M+H]^+$: 2093.09), *m/z* 1047.15 (calcd mass for $C_{89}H_{155}N_{21}O_{36}$ $[M+2H]^{2+}$: 1047.05).

5''-Amino-5''-deoxy-Boc-protected guanidinoneomycin derivative (6). To a solution of compound **5** (182 mg, 0.086 mmol) in MeOH (1 mL), Pd/C (10 wt % on activated carbon, 46 mg, 0.04 mmol) was added. The mixture was stirred under an atmosphere of hydrogen for 17 h at RT. The catalyst was removed by filtration through Celite, and the filtrate was concentrated *in vacuo*. Purification by silica gel flash-column chromatography (gradient: 0-10 % of MeOH in DCM) afforded the desired product as a white solid (71 mg, 40%). R_f (5% MeOH in DCM): 0.40; ESI MS, positive mode: *m/z* 2066.85 (calcd mass for $C_{89}H_{156}N_{19}O_{36}$ $[M+H]^+$: 2067.09), *m/z* 1033.90 (calcd mass for $C_{89}H_{157}N_{19}O_{36}$ $[M+2H]^{2+}$: 1034.05).

Synthesis and characterization of conjugates 8 and 9.

Boc-protected Pt-guanidinoneomycin conjugate (7). A solution of *trans,trans,trans*-$[Pt(N_3)_2(OH)(succ)(py)_2]$ (6.11 mg, 10.7 µmol) and DIPEA (25 µL, 143 µmol) in freshly N_2-bubbled anhydrous DMF (500 µL) was added under an Ar atmosphere to an Eppendorf tube containing solid HATU (3.5 mg, 9.2 µmol). After stirring for 3 min under Ar, the resulting yellow mixture was added to a solution of the Boc-protected amino derivative of guanidinoneomycin **6** (15.1 mg, 7.3 µmol) in anhydrous DMF (500 µL) and DIPEA (15 µL, 86 µmol). The reaction mixture was stirred for 2 h at RT under an Ar atmosphere. After evaporation *in vacuo,* purification by silica gel flash-column chromatography (gradient: 0-8.5 % of MeOH in DCM) afforded the desired product as a white solid (17 mg, 89%). R_f (5% MeOH in DCM): 0.75; HR ESI-MS, positive mode: *m/z* 1310.5886 (calcd mass for $C_{103}H_{171}N_{27}O_{40}Pt$ $[M+2H]^{2+}$: 1310.5906), *m/z* 874.0611 (calcd mass for $C_{103}H_{172}N_{27}O_{40}Pt$ $[M+3H]^{3+}$: 874.0628).

Pt-guanidinoneomycin conjugate (8). Boc-protected conjugate **7** (5 mg, 2 µmol) was dissolved in a 1:1 (v/v) mixture of TFA/DCM and stirred for 2 h at room temperature protected from light. The reaction mixture was concentrated *in vacuo* and after several co-evaporations with toluene and DCM, the crude was dissolved in water and lyophilized. Purification by analytical HPLC afforded the trifluoroacetate salt of conjugate **8** as a yellow solid (1.5 mg, 34%). Characterization: R_t= 15.7 min (analytical gradient: 0 to 100% B in 30 min); HR ESI MS, positive mode: *m/z* 793.7551 (calcd mass for $C_{47}H_{74}F_6N_{24}O_{19}Pt$ $[M+2H]^{2+}$: 793.7552), *m/z* 529.5060 (calcd mass for $C_{47}H_{75}F_6N_{24}O_{19}Pt$ $[M+3H]^{3+}$: 529.5059); ^{1}H NMR (500 MHz, D_2O), δ (ppm): 8.72 (4H, H_{ortho} *py*, d, *J* = 6.0 Hz), 8.20 (2H, H_{para} *py*, t, *J* = 7.5 Hz), 7.71 (4H, H_{meta} *py*, t, *J* = 6.7 Hz), 5.57 (1H, d, *J* = 4.0 Hz), 4.98 (1H, d, *J* = 2.0 Hz), 4.90 (1H, br s), 4.19 (1H, m), 4.12 (1H, t, *J* = 5.5 Hz), 4.01 (1H, t, *J* = 2.7 Hz), 3.98 (1H, t, *J* = 6.7 Hz), 3.83 (1H, q, *J* = 5.5 Hz), 3.67–3.58 (4H, m), 3.51–3.44 (5H, m), 3.40–3.28 (8H, m), 3.22 (1H, m), 2.67 (2H, t, *J* = 6.7 Hz), 2.35 (2H, t, *J* = 6.7 Hz), 2.11 (1H, dt, *J* = 12.0 Hz), 1.53 (1H, q, *J* = 12.0 Hz). ^{19}F NMR (376 MHz, D_2O), δ (ppm): -76.1 ppm (6F, br). The ^{195}Pt NMR could not be recorded due to sample limitation.

Pt-guanidinoneomycin conjugate (9). Compound **6** (4 mg, 2 µmol) was deprotected with TFA/DCM 1:1 (1 mL) for 2 h at RT. The reaction mixture was evaporated *in vacuo* and after several co-evaporations with toluene

and DCM, the trifluoroacetate salt of 5''-amino-5''-deoxy-guanidinoneomycin was obtained. On the other hand, a solution of complex **3** (1.8 mg, 3.1 µmol) and DIPEA (2 µL, 11.4 µmol) in freshly N_2-bubbled anhydrous DMF (100 µL) was added under an Ar atmosphere to an Eppendorf tube containing solid HATU (1.0 mg, 2.6 µmol). After stirring for 3 min under Ar, the resulting yellow mixture was added to a solution of the deprotected 5''-amino-5''-deoxy-guanidinoneomycin in anhydrous DMF (100 µL) and DIPEA (3 µL, 17 µmol). The reaction mixture was stirred for 2 h at RT under an Ar atmosphere. After evaporation *in vacuo,* the crude was dissolved in water and lyophilized. Purification by analytical HPLC afforded the trifluoroacetate salt of conjugate **9** as a yellow solid (1.20 mg, 29%). The synthesis was repeated two more times to get enough sample for cellular uptake and phototoxicity studies. Characterization: R_t = 12.0 min (analytical gradient: 0 to 100% B in 30 min); HR ESI MS, positive mode: *m/z* 710.2765 (calcd mass for $C_{43}H_{75}N_{27}O_{16}Pt$ $[M+2H]^{2+}$: 710.2760), *m/z* 473.8529 (calcd mass for $C_{43}H_{76}N_{27}O_{16}Pt$ $[M+3H]^{3+}$: 473.8531); ^{1}H NMR (500 MHz, D_2O), δ (ppm): 8.66 (4H, H_{ortho} *py*, d, *J* = 5.5 Hz), 8.18 (2H, H_{para} *py*, t, *J* = 8.0 Hz), 7.70 (4H, H_{meta} *py*, t, *J* = 7.0 Hz), 5.56 (1H, d, *J* = 3.0 Hz), 4.96 (1H, d, *J* = 2.0 Hz), 4.90 (1H, br s), 4.20 (1H, m), 4.13 (1H, t, *J* = 5.5 Hz), 4.02 (1H, t, *J* = 3.0 Hz), 3.99 (1H, m), 3.84 (1H, q, *J* = 5.5 Hz), 3.67–3.57 (5H, m), 3.50–3.42 (4H, m), 3.39–3.26 (8H, m), 3.22 (1H, m), 2.58 (2H, t, *J* = 7.0 Hz), 2.35 (2H, t, *J* = 7.0 Hz), 2.11 (1H, dt, *J* = 12.5 Hz), 1.53 (1H, q, *J* = 12.5 Hz). The ^{195}Pt NMR could not be recorded due to sample limitation.

Reactivity of complexes 2 and 3 with TFA; synthesis and characterization of complexes 10 and 11.

trans,trans,trans-[Pt(N$_3$)$_2$(CF$_3$COO)$_2$(py)$_2$] (10)

Complex **2** (*trans,trans,trans*-$Pt(N_3)_2(OH)_2(pyr)_2$][6a] (0.04 g, 0.085 mmol) was dissolved in a 1:1 mixture of TFA/anhydrous DCM (1 mL) and allowed to react for 2 h at room temperature protected from light. The solvent was evaporated and the crude solid was purified via silica gel chromatography, using DCM as an eluent, which afforded complex **10** as a yellow solid (22 mg, 39%). Crystals suitable for X-ray diffraction were formed by the slow evaporation of a concentrated solution of **10** in DCM at room temperature overnight. Complex **10** has extremely low solubility in water (0.40 µM in 10% DMSO and 0.25 µM in 5% DMSO as calculated by ICP-MS analysis). Characterization: R_f (DCM): 0.40; HR ESI MS, positive mode: *m/z* 686.0268 (calcd mass for $C_{14}H_{10}F_6N_8NaO_4Pt$ $[M+Na]^+$: 686.0270); ^{1}H NMR (500 MHz, CD_3OD), δ (ppm): 8.94 (4H, H_{ortho}, dd, $^3J_{1H1H}$ = 5.7 Hz, $^3J_{195Pt1H}$ = 25.2 Hz), 8.30 (2H, H_{para}, t, $^3J_{1H1H}$ = 7.4 Hz,), 7.90 (4H, H_{meta}, t, $^3J_{1H1H}$ = 7.0 Hz); ^{195}Pt NMR (107 MHz, CD_3OD), δ (ppm): 1233; ^{19}F NMR (376 MHz, CD_3OD), δ (ppm): -76.0 (6F, d, $^4J_{195Pt19F}$ = 5.1 Hz); ^{13}C NMR (125 MHz, CD_3OD), δ (ppm): 150.8 (C_{ortho}), 144.4 (C_{para}), 128.2 (C_{meta}, $^3J_{195Pt13C}$= 12.5 Hz). The tertiary trifluoroacetate carbons were not observed after 16384 scans.

trans,trans,trans-[Pt(N$_3$)(CF$_3$COO)(succ)(CF$_3$COO)(py)$_2$)] (11)

Complex **3** (*trans,trans,trans*-$Pt(N_3)_2(OH)(succ)(pyr)_2$][20] (0.023 g, 0.040 mmol) was dissolved in a 1:1 mixture of TFA/anhydrous DCM (560 µL) and allowed to react for 2 h at room temperature protected from light. The solvent was then removed and purification was carried out via silica gel chromatography using as an eluent a 9:1 (v/v) mixture of DCM/MeOH. The pure product was dissolved in the minimum amount of DCM and hexane was added to induce the precipitation. Complex **11** was obtained as a yellow solid (14 mg, 48%). Crystals suitable for X-ray diffraction were formed upon the slow evaporation of a concentrated solution of **11** in 10% MeOH/ 90% DCM at room temperature. The complex is soluble in a variety of solvents (e.g. diethyl ether, ethanol, methanol, acetone) although when the sample was left standing in methanol for 24 days, decomposition was observed (25% by NMR). Characterization: R_f (DCM/MeOH 9:1): 0.25; HR ESI MS, positive mode: *m/z* 761.0365 (calcd mass for $C_{18}H_{15}F_6N_5NaO_8Pt$ $[M+Na]^+$: 761.0366); ^{1}H NMR (400 MHz, acetone-d_6), δ (ppm): 8.9 (4H, H_{ortho}, dd, $^3J_{1H1H}$ = 5.9 Hz, $^3J_{195Pt1H}$ = 12.0 Hz), 8.4 (2H, H_{para}, t, $^3J_{1H1H}$ = 7.4 Hz), 7.9 (4H, H_{meta}, t, $^3J_{1H1H}$ = 7.7 Hz), 2.6 (2H, H_{succ}, t, $^3J_{1H1H}$ = 6.9 Hz), 2.5 (2H, H_{succ}, t, $^3J_{1H1H}$ = 6.9 Hz); ^{195}Pt NMR (107 MHz, CD_3OD), δ (ppm): 1611; ^{19}F NMR (376 MHz, CD_3OD), δ (ppm): -76.1 ppm (3F, d, $^4J_{195Pt19F}$ = 3.0 Hz, TFA axial or equatorial), -76.2 ppm (3F, d, $^4J_{195Pt19F}$ = 4.2 Hz, TFA axial or equatorial); ^{13}C NMR (125 MHz, CD_3OD), δ (ppm): 150.0 (C_{ortho}), 144.0 (C_{para}), 127.8 (C_{meta}, $^3J_{195Pt13C}$= 12.4 Hz), 177.9 (-C=O, C_{succ}), 176.1 (-C=O, C_{succ}), 31.2 (-CH_2-, C_{succ}), 30.9 (-CH_2-, C_{succ}). The tertiary trifluoroacetate carbons were not observed after 16384 scans.

Photoreactions with 5'-guanosine monophosphate. The required volume of an aqueous solution of conjugate **8** or **9** (20 nmol) was mixed with the required volume of an aqueous solution of 5'-GMP (2 mol equiv). The solutions were 35 µM in the conjugates. Platination reactions were carried out at 310 K in a 0.1 cm path-length quartz cuvette under visible light irradiation. The light source was a Philips Belgium A3 Master HPI-T Plus 100W visible lamp and a 1 M aqueous solution of $NaNO_2$ was used as a filter to cut off the UV-light and ensure the appropriate wavelength range (> 400 nm). The evolution of the reactions was monitored by reversed-phase HPLC on a Jupiter Proteo column (250x4.6 mm, 4 µm, flow rate: 1 mL/min), using linear gradients of 0.045% TFA in H_2O (solvent A) and 0.036% TFA in ACN (solvent B). Platinum adducts were isolated after several HPLC runs by using analytical separation conditions and characterized by HR ESI-MS. Adduct *trans*-$[Pt(N_3)(py)_2(5'\text{-GMP})]^+$ (**12**). HR ESI MS, positive mode: *m/z* 758.1142 (calcd mass for $C_{20}H_{24}N_{10}O_8PPt$ $[M]^+$: 758.1164). Adduct *trans*-$[Pt(py)_2(5'\text{-GMP})_2]^{2+}$ (**13**). HR ESI MS, positive mode: *m/z* 1078.1575 (calcd mass for $C_{30}H_{37}N_{12}O_{16}P_2Pt$ $[M-H]^+$: 1078.1573).

Photoreactions with $^{5'}$dCATGGCT. *A) Reactions with single-stranded oligonucleotide.* A solution (300 µL) of $^{5'}$dCATGGCT (7.5 nmol) in 10 mM phosphate buffer, pH = 6.8, was added either over lyophilized conjugate **9** (4 mol equiv) or over complex **3** (2 mol equiv). The resulting solutions (25 µM in the oligonucleotide) were transferred into quartz cuvettes and irradiated under visible light for 24 h at 310 K as indicated above. *B) Analysis and characterization of the platinum adducts:* The evolution of the reactions was monitored by reversed-phase HPLC on a Jupiter C_{18} column (250 x 4.6 mm, 5 µm, flow rate: 1 mL/min, detection wavelength: 260 nm), using linear gradients of aqueous triethylammonium acetate (0.05 M) (solvent A) and ACN/H_2O 1:1 (solvent B). Platinum adducts were isolated after several HPLC runs by using analytical separation conditions. HR MALDI-TOF MS analysis was carried out in the positive or negative mode using 2,4,6-trihidroxyacetophenone matrix with ammonium citrate as an additive. Enzymatic digestions with 5'- and 3'-exonucleases (bovine spleen and snake venom phosphodiesterases, respectively) were performed as previously described.[27,28] *B.1) Adduct $^{5'}$dCATG**G**CT-{PtN$_3$(py)$_2$}$^+$* ***15a***: R_t= 25.1 min (gradient: 0 to 50% B in 40 min). MALDI-TOF-MS, positive mode: *m/z* 2490.6 (calcd mass for $C_{78}H_{97}N_{30}O_{41}P_6Pt$ $[M]^+$: 2490.45). MALDI-TOF-MS, negative mode, after digestion with snake venom phosphodiesterase: *m/z* 1894.8 (-pCpT) (calcd mass for $C_{59}H_{70}N_{25}O_{28}P_4Pt$ $[M-2H]^-$: 1895.34). MALDI-TOF-MS, negative mode, after digestion with bovine spleen phosphodiesterase: *m/z* 1581.9 (-CpApTp) (calcd mass for $C_{49}H_{58}N_{20}O_{23}P_3Pt$ $[M-2H]^-$: 1582.28), *m/z* 1252.9 (-CpApTpGp) (calcd mass for $C_{39}H_{46}N_{15}O_{17}P_2Pt$ $[M-2H]^-$: 1253.23). *B.2) Adduct $^{5'}$dCAT**G**GCT-{PtN$_3$(py)$_2$}$^+$* ***15b***: R_t= 25.5 min (gradient: 0 to 50% B in 40 min). MALDI-TOF-MS, positive mode: *m/z* 2490.5 (calcd mass for $C_{78}H_{97}N_{30}O_{41}P_6Pt$ $[M]^+$: 2490.45). MALDI-TOF-MS, negative mode, after digestion with snake venom phosphodiesterase: *m/z* 1565.8 (-pGpCpT) (calcd mass for $C_{49}H_{58}N_{20}O_{22}P_3Pt$ $[M-2H]^-$: 1566.29). MALDI-TOF-MS, negative mode, after digestion with bovine spleen phosphodiesterase: *m/z* 1885.8 (-CpAp) (calcd mass for $C_{59}H_{71}N_{22}O_{30}P_4Pt$ $[M-2H]^-$: 1886.33), *m/z* 1581.9 (-CpApTp) (calcd mass for $C_{49}H_{58}N_{20}O_{23}P_3Pt$ $[M-2H]^-$: 1582.28). *B.3) Adduct $^{5'}$dCAT**GG**CT-{PtN$_3$(py)$_2$}$_2^{2+}$* ***15c***: R_t= 31.0 min (gradient: 0 to 50% B in 40 min). MALDI-TOF-MS, positive mode: *m/z* 2884.5 (calcd mass for $C_{88}H_{106}N_{35}O_{41}P_6Pt_2$ $[M-H]^+$: 2884.50), *m/z* 2490.5 (calcd mass for $C_{78}H_{97}N_{30}O_{41}P_6Pt$ $[M-\{PtN_3(py)_2\}]^+$: 2490.45). MALDI-TOF-MS, negative mode, after digestion with snake venom phosphodiesterase:

m/z 2289.8 (-pCpT) (calcd mass for $C_{69}H_{79}N_{30}O_{28}P_4Pt_2$ [M-3H]$^-$: 2289.39), *m/z* 1894.8 (-pCpT) (calcd mass for $C_{59}H_{70}N_{25}O_{28}P_4Pt$ [M-{$PtN_3(py)_2$}-2H]$^-$: 1895.34). MALDI-TOF-MS, negative mode, after digestion with bovine spleen phosphodiesterase: *m/z* 2279.4 (-CpAp) (calcd mass for $C_{69}H_{80}N_{27}O_{30}P_4Pt_2$ [M-3H]$^-$: 2280.38), *m/z* 1885.8 (-CpAp) (calcd mass for $C_{59}H_{71}N_{22}O_{30}P_4Pt$ [M-{$PtN_3(py)_2$}-2H]$^-$: 1886.33), *m/z* 1581.8 (-CpApTp) (calcd mass for $C_{49}H_{58}N_{20}O_{23}P_3Pt$ [M-{$PtN_3(py)_2$}-2H]$^-$: 1582.28).

Phototoxicity studies. Cell culture media and other chemicals were obtained from Sigma-Aldrich Ltd (Poole, UK). Disposable sterile cell culture plastics were obtained from Greiner Bio-One (Cambridge, UK). All procedures were carried out in a specially adapted photobiology laboratory with ambient light levels measured below 1 lux (Solatell, UK). Phototoxicity was determined according to the OECD 432 guideline with some modification as described below. DU-145 human prostate carcinoma cells and SK-MEL-28 human melanoma cells were obtained from the European Collection of Cell Cultures (Porton Down, UK) and maintained in DMEM containing 10% (v/v) foetal calf serum according to instructions. Cells were mycoplasma free and maintained in antibiotic-free conditions in a humidified atmosphere of 5% CO_2/95% air. For experiments, cells were seeded at a density of 6-7 x 10^4cells/cm^2 in 96-well plates. Compounds were prepared immediately before use in optically clear Earle' Balanced Salt Solution (EBSS) and filter sterilized. The compounds were incubated with the cells for 60 min prior to irradiation. Irradiations were immediately performed in optically-clear medium and experiments were controlled for light, complex, and handling. Visible light (5 J/cm^2) was delivered by a bank of TL03 fluorescent tubes (λ_{max}: 420 nm) with wavelengths shorter than 400 nm blocked by filtering. The irradiation time was 60-70 min. Irradiance was measured with a Gigahertz Optik meter calibrated to the source using a spectroradiometer (Bentham Instruments Ltd, UK; mean irradiance 1.3 mW/cm^2 ± 0.1). Sham-irradiated cells were treated identically and in parallel with irradiated cells, except that photons were blocked. The viability of DU-145 cells irradiated with visible light was 102.5 ± 6.7%; and of SK-MEL-28 cells was 101.3 ± 6.9%.

Phototoxicity was determined by neutral red dye uptake 24 h after irradiation. The absorbance of the neutral red dye was read at 540 nm in a Synergy™ 2 plate reader. The concentration of compound required to inhibit dye uptake by 50% (IC_{50} value) was calculated using non-linear regression from the log-transformed cytotoxicity curves normalised to untreated cells (Graphpad Prism v.6). Goodness of fit was determined by the 95% confidence interval of the IC_{50} value, and the R^2 value. The results represent the mean and error of at 2/3 independent experiments performed in triplicate.

Platinum accumulation in cancer cells. For platinum cellular uptake studies, about 1.0 x10^6 SK-MEL-28 and DU-145 cells were plated in 100 mm Petri dishes and allowed to attach for 24 h. Next, the plates were exposed to *trans,trans,trans*-[$Pt(N_3)_2(OH)_2(py)_2$] (**2**), *trans,trans,trans*-[$Pt(N_3)_2(OH)(succ)(py)_2$] (**3**) or to the Pt^{IV}-guanidinoneomycin conjugate (**9**) at a 10 μM concentration. Additional plates were incubated with medium alone as negative control. After 1 h of incubation in the dark at 310 K, the cells were rinsed three times with cold PBS and harvested by trypsinization. The number of cells in each sample was counted manually in a haemocytometer using the trypan blue dye exclusion test. Then the cells were centrifuged to obtain the whole cell pellet for ICP-MS analysis. All experiments were conducted in triplicate.

ICP-MS analysis. The whole cell pellets were dissolved in 500 μL of concentrated 72% v/v nitric acid, and the samples were then transferred into wheaton v-vials (Sigma-Aldrich) and heated in an oven at 373 K for 18 h. The vials were then allowed to cool, and each cellular sample solution was transferred into a volumetric tube and combined with washings with Milli-Q water (1.5 mL). Digested samples were diluted 5 times with Milli-Q to obtain a final HNO_3 concentration of approximately 3.6% v/v. Platinum content was analyzed on an ICP-MS Perkin Elmer Elan 6000 series instrument at the Centres Científics i Tecnològics of the Universitat de Barcelona. The solvent used for all ICP-MS experiments was Milli-Q water with 1% HNO_3. The platinum standard (High-Purity Standards, 1000 μg/mL $\pm$ 5 μg/mL in 5% HNO_3) was diluted with 1% HNO_3 to 20 ppb. Platinum standards were freshly prepared in Milli-Q water with 1% HNO_3 before each experiment. The concentrations used for the calibration curve were in all cases 0, 0.2, 0.4, 1, and 2 ppb. The isotope detected was ^{196}Pt and readings were made in triplicate. Rhodium was added as an internal standard at a concentration of 10 ppb in all samples.

Acknowledgements

This work was supported by funds from the Spanish *Ministerio de Economía y Competitividad* (grants CTQ2010-21567-C02-01-02, CTQ2014-52658-R and the RNAREG project, grant CSD2009-00080), the *Generalitat de Catalunya* (2009SGR-208 and the *Xarxa de Referència de Biotecnologia*), the ERC (grant 247450), EPSRC (EP/F034210/1) and EPSRC (MOAC Doctoral Training Centre, EP/F500378/1). We acknowledge helpful assistance of Dr. Mª Antonia Molins and Dr. Francisco Cárdenas (NMR), Dr Maite Romero (ICP-MS) and Dr. Irene Fernández and Laura Ortiz (MS) from *Centres Científics i Tecnològics* of the University of Barcelona.

Keywords: anticancer agents • platinum • photoactivation • DNA binding • guanidinoneomycin

[1] a) P. J. Dyson, G. Sava, *Dalton Trans*. **2006**, 1929-1933; b) L. Kelland, *Nat Rev Cancer* **2007**, *7*, 573-584; c) N. J. Wheate, S. Walker, G. E. Craig, R. Oun, *Dalton Trans*. **2010**, *39*, 8113-8127; d) B. W. Harper, A. M. Krause-Heuer, M. P. Grant, M. Manohar, K. B. Garbutcheon-Singh, J. R. Aldrich-Wright, *Chem. Eur. J*. **2010**, *16*, 7064-7077; e) S. Dasari, P. Bernard Tchounwou, *Eur. J. Pharmacol.* **2014**, *740*, 364-378.

[2] a) N. J. Farrer, L. Salassa, P. J. Sadler, *Dalton Trans*. **2009**, 10690-10701; b) D. Crespy, K. Landfester, U. S. Schubert, A. Schiller, *Chem. Commun*. **2010**, *46*, 6651-6662; c) U. Schatzschneider, *Eur. J. Inorg. Chem*. **2010**, *10*, 1451-1467; d) E. C. Glazer, *Isr. J. Chem*. **2013**, *53*, 391-400.

[3] a) M. D. Hall, H. R. Mellor, R. Callaghan, T. W. Hambley, *J. Med. Chem*. **2007**, *50*, 3403-3411; b) J. J. Wilson, S. J. Lippard, *Chem. Rev.* **2014**, *114*, 4470-4495; c) E. Wexselblatt, D. Gibson, *J. Inorg. Biochem.* **2012**, *117*, 220-229; d) E. Gabano, M. Ravera, D. Osella, *Dalton Trans*. **2014**, *43*, 9813-9820.

[4] a) S. J. Berners-Price, *Angew. Chem. Int. Ed*. **2011**, *50*, 804-805; b) E. Shaili, *Sci. Prog*. **2014**, *97*, 20-40.

[5] F. S. Mackay, J. A. Woods, P. Heringova, J. Kasparkova, A. M. Pizarro, S. A. Moggach, S. Parsons, V. Brabec, P. J. Sadler, *Proc. Nat. Acad. Sci. U.S.A.* **2007**, *104*, 20743-20748.

[6] a) N. J. Farrer, J. A. Woods, L. Salassa, Y. Zhao, K. S. Robinson, G. Clarkson, F. S. Mackay, P. J. Sadler, *Angew. Chem. Int. Ed*. **2010**, *49*, 8905-8908; b) J. S. Butler, J. A. Woods, N. J. Farrer, M. E. Newton, P. J. Sadler, *J. Am. Chem. Soc*. **2012**, *134*, 16508-16511.

[7] a) Y. Zhao, J. A. Woods, N. J. Farrer, K. S. Robinson, J. Pracharova, J. Kasparkova, O. Novakova, H. Li, L. Salassa, A. M. Pizarro, G. J. Clarkson, L. Song, V. Brabec, P. J. Sadler, *Chem. Eur. J.* **2013**, *19*, 9578-9591; b) Y. Zhao, N. J. Farrer, H. Li, J. S. Butler, R. J. McQuitty, A. Habtemariam, F. Wang, P. J. Sadler, *Angew. Chem. Int. Ed*. **2013**, *52*, 13633-13637; c) A. M. Pizarro, R. J. McQuitty, F. S. Mackay, Y. Zhao, J. A. Woods, P. J. Sadler, *ChemMedChem* **2014**, *9*, 1169-1175.

[8] a) H.-C. Tai, R. Brodbeck, J. Kasparkova, N. J. Farrer, V. Brabec, P. J. Sadler, R. Deeth, *J. Inorg. Chem*. **2012**, *51*, 6830-6841; b) J. Pracharova, L. Zerzankova, J. Stepankova, O. Novakova, N. J. Farrer, P. J. Sadler, V. Brabec, J. Kasparkova, *Chem. Res. Toxicol*. **2012**, *25*, 1099-1111.

[9] a) S. Betanzos-Lara, L. Salassa, A. Habtemanriam, P. J. Sadler, *Chem. Commun*. **2009**, 6622-6624; b) F. Barragán, P. López-Senín, L. Salassa, S. Betanzos-Lara, A. Habtemariam, V. Moreno, P. J. Sadler, V. Marchán, *J. Am. Chem. Soc*. **2011**, *133*, 14098-14108; c) L. Salassa, *Eur. J. Inorg. Chem*. **2011**, 4931-4947; d) R. E. Goldbach, I. Rodriguez-Garcia, J. H. van Lenthe, M. A. Siegler, S. Bonnet, *Chem. Eur. J*. **2011**, *17*, 9924-9929; e) E. Wachter, D. K. Heidary, B. S. Howerton, S. Parkin, E. C. Glazer, *Chem. Commun*. **2012**, 9649-9651; f) B. S. Howerton, D. K. Heidary, E. C. Glazer, *J. Am. Chem. Soc*. **2012**, *134*, 8324-8327; g) A. Kastl, A. Wilbuer, A. L. Merkel, L. Feng, P. Di Fazio, M. Ocker, E. Meggers, *Chem. Commun*. **2012**, 1863-1865; h) S. H. C. Askes, A. Bahreman, S. Bonnet, *Angew. Chem. Int. Ed*. **2014**, *53*, 1029-1033; i) E. Ruggiero, A. Habtemariam, L. Yate, J. C. Mareque-Rivas, L. Salassa, *Chem. Commun*. **2014**, 1715-1718; j) A. Leonidova, V. Pierroz, R. Rubbiani, J. Heier, S. Ferrari, G. Gasser, *Dalton Trans*. **2014**, *43*, 4287-4294; k) Z. Li, A. David, B. A. Albani, J.-P. Pellois, C. Turro, K. R. Dunbar, *J. Am. Chem. Soc*. **2014**, *136*, 17058-17070; l) K. Waehler, A. Ludewig, P. Szabo, K. Harms, E. Meggers, *Eur. J. Inorg. Chem.* **2014**, 807-811; m) C. Mari, V. Pierroz, S. Ferrari, G. Gasser, *Chem. Sci*. **2015**, *6*, 2660-2686; n) T. K. Goswami, S. Gadadhar, B. Balaji, B. Gole, A. A. Karande, A. R. Chakravarty, *Dalton Trans*. **2014**, *43*, 11988-11999; o) S. Banerjee, I. Pant, I. Khan, P. Prasad, A. Hussain, P. Kondaiah, A. R. Chakravarty, *Dalton Trans*. **2015**, *44*, 4108-4122.

[10] T. Joshi, V. Pierroz, C. Mari, L. Gemperle, S. Ferrari, G. Gasser, *Angew. Chem. Int. Ed*. **2014**, *53*, 2960-2963.

[11] A. Leonidova, V. Pierroz, R. Rubbiani, Y. Lan, A. G. Schmitz, A. Kaech, R. K. O. Sigel, S. Ferrari, G. Gasser, *Chem. Sci*. **2014**, *5*, 4044-4056.

[12] a) X. Wang, Z. Guo, *Chem. Soc. Rev*. **2013**, *42*, 202-224; b) J. S. Butler, P. J. Sadler, *Curr. Opin. Chem. Biol*. **2013**, *17*, 175-188.

[13] a) K. R. Barnes, A. Kutikov, S. J. Lippard, *Chem. Biol.* **2004**, *11*, 557-564; b) S. Dhar, Z. Liu, J. Thomale, H. Dai, S. J. Lippard, *J. Am. Chem. Soc*. **2008**, *130*, 11467-11476; c) S. Mukhopadhyay, C. M. Barnés, A. Haskel, S. M. Short, K. R. Barnes, S. J. Lippard, *Bioconjugate Chem*. **2008**, *19*, 39-49; d) S. Abramkin, S. M. Valiahdi, M. A. Jakupec, M. Galanski, N. Metzler-Nolte, B. K. Keppler, *Dalton. Trans*. **2012**, *41*, 3001-3005; e) A. Massaguer, A. González-Cantó, E. Escribano, S. Barrabés, G. Artigas, V. Moreno, V. Marchán, *Dalton Trans*. **2015**, *44*, 202-212; f) A. Gandioso, E. Shaili, A. Massaguer, G. Artigas, A. González-Cantó, J. A. Woods, P. J. Sadler, V, Marchán, *Chem. Commun*. **2015**, *51*, 9169-9172.

[14] a) Y. Dai, H. Xiao, J. Liu, Q. Yuan, P. Ma, D. Yang, C. Li, Z. Cheng, Z. Hou, P. Yang, J. Lin, *J. Am. Chem. Soc*. **2013**, *135*, 18920-18929; b) Y. Min, J. Li, F. Liu, E. K. Yeow, B. Xing, *Angew. Chem. Int. Ed*. **2014**, *53*, 1012-1016.

[15] N. Graf, S. J. Lippard, *Adv. Drug Deliv. Rev*. **2012**, *64*, 993-1004.

[16] a) N. W. Luedtke, T. J. Baker, M. Goodman, Y. Tor, *J. Am. Chem. Soc*. **2000**, *122*, 12035-12036; b) E. G. Stanzl, B. M. Trantow, J. R. Vargas, P. A. Wender, *Acc. Chem. Res.* **2013**, *46*, 2944-2954; c) E. Wexselblatt, J. D. Esko, Y. Tor, *J. Org. Chem*. **2014**, *79*, 6766.-6774.

[17] a) N. W. Luedtke, P. Carmichael, Y. Tor, *J. Am. Chem. Soc*. **2003**, *125*, 12374-12375; b) J. L. Houghton, K. D. Green, W. Chen, S. Garneau-Tsodikova, *ChemBioChem*, **2010**, *11*, 880-902.

[18] a) L. Elson-Schwab, O. B. Garner, M. Schuksz, B. E. Crawford, J. D. Esko, Y. Tor, *J. Biol. Chem.* **2007**, *282*, 13585-13591; b) S. Sarrazin, B. Wilson, W. S. Sly, Y. Tor, J. D. Esko, *Mol. Ther.* **2010**, *18*, 1268-1274; c) M. Inoue, W. Tong, J. D. Esko, Y. Tor, *ACS Chem. Biol.* **2013**, *8*, 1383-1388; d) M. Inoue, E. Wexselblatt, J. D. Esko, Y. Tor, *ChemBioChem* **2014**, *15*, 676-680.

[19] A. Grau-Campistany, A. Massaguer, D. Carrion-Salip, F. Barragán, G. Artigas, P. López-Senín, V. Moreno, V. Marchán, *Mol. Pharmaceutics* **2013**, *10*, 1964-1976.

[20] E. Shaili, Ph.D. Thesis, University of Warwick, **2013**.

[21] J. Boer, K. F. Blount, N. W. Luedtke, L. Elson-Schwab, Y. Tor, *Angew. Chem., Int. Ed*. **2005**, *44*, 927-932.

[22] M. S. Bernatowicz, Y. Wu, G. R. Matsueda, *Tetrahedron Lett*. **1993**, *34*, 3389-3392.

[23] F. S. Mackay, S. A. Moggach, A. Collins, S. Parsons, P. J. Sadler, *Inorg. Chim. Acta* **2009**, *362*, 811-819.

[24] Y.-E. Kwon, K.-J. Whang, Y.-J.; Park, K. H. Kim, *Bioorg. Med. Chem*. **2003**, *11*, 1669-1676.

[25] a) E. Wexselblatt, R. Raveendran, S. Salameh, A. Friedman-Ezra, E. Yavin, D. Gibson, *Chem. Eur. J.* **2015**, *21*, 3108-3114; b) E. Wexselblatt, E. Yavin, D. Gibson, *Angew. Chem. Int. Ed*. **2013**, *52*, 6059-6062.

[26] L. Ronconi, A. M. Pizarro, R. J. McQuitty, P.J. Sadler, *Chem. Eur. J*. **2011**, *17*, 12051-12059.

[27] a) F. Barragán, V. Moreno, V. Marchán, *Chem. Commun*. **2009**, 4705-4707; b) F. Barragán, D. Carrion, I. Gómez-Pinto, A. González-Cantó, P. J. Sadler, R. de Llorens, V. Moreno, C. González, A. Massaguer, V. Marchán, *Bioconjugate Chem*. **2012**, *23*, 1838-1855.

[28] a) V. Marchán, E. Pedroso, A. Grandas, *Chem.Eur. J*. **2004**, *10*, 5369-5375; b) B. Algueró, J. López de la Osa, C. González, E. Pedroso, V. Marchán, A. Grandas, *Angew. Chem., Int. Ed*. **2006**, *45*, 8194-8197; c) B. Algueró, E. Pedroso, V. Marchán, A. Grandas, *J. Biol. Inorg. Chem*. **2007**, *12*, 901-911.

[29] a) A. E. Egger, C. Rappel, M. A. Jakypec, C. G. Hartinger, P. Heffeter, B. K. Keppler, *J. Anal. At. Spectrom.* **2009**, *24*, 51-61; b) A. Ghezzi, M. Aceto, C. Cassino, E. Gabano, D. Osella, *J. Inorg. Biochem*. **2004**, *98*, 73-78; c) A. R. Timerbaev, *J. Anal. At. Spectrom*. **2014**, *29*, 1058-1072.

[30] a) H. Silva, F. Frézard, E. J. Peterson, P. Kabolizadeh, J. J. Ryan, N. P. Farrell, *Mol. Pharmaceut.* **2012**, *9*, 1795-1802; b) S. M. Fuchs, R. T. Raines, *Cell. Mol. Life Sci*. **2006**, *63*, 1819-1822.

[31] a) J. R. Bishop, M. Schuksz, J. D. Esko, *Nature* **2007**, *446*, 1030-1037; b) A. Walrant, C. Bechara, I. D. Alves, S. Sagan, *Nanomedicine* **2012**, *7*, 133-143. c) M. Belting, *Trends Biochem. Sci*. **2003**, *28*, 145-151. d) J. D. Esko, U. Lindahl, *J. Clin. Invest*. **2001**, *108*, 169-173.

[32] A. J. Eustace, J. Crown, M. Clynes, N. O'Donovan, *J. Transl. Med*. **2008**, *6*, 53-63.

[33] a) Y. Tor, *ChemBioChem*. **2003**, *4*, 998-1007; b) J. R. Thomas, P. J. Hergenrother, *Chem. Rev*. **2008**, *108*, 1171-1224; c) M. Chittapragada, S. Roberts, Y. W. Ham, *Perspect. Med. Chem*. **2009**, *3*, 21-37; d) J. L. Houghton, K. D. Green, W. Chen, S. Garneau-Tsodikova, *ChemBioChem* **2010**, *11*, 880-902.

[34] a) J. D. White, M. F. Osborn, A. D. Moghaddam, L. E. Guzman, M. M. Haley, V. J. DeRose, *J. Am. Chem. Soc*. **2013**, *135*, 11680-11683; b) M. F. Osborn, J. D. White, M. M. Haley, V. J. DeRose, *ACS Chem. Biol*. **2014**, *9*, 2404-2411; c) K. Rijal, X. Bao, C. S. Chow, *Chem. Commun*. **2014**, 3918-3920; d) K. Rijal, C. S. Chow, *Chem. Commun*. **2009**, 107-109; e) A. A. Hostetter, E. G. Chapman, V. J. DeRose, *J. Am. Chem. Soc*. **2009**, *131*, 9250-9257; f) E. G. Chapman, V. J. DeRose, *J. Am. Chem. Soc*. **2012**, *134*, 256-262.

[35] O. V. Dolomanov, L. J. Bourhis, R. J. Gildea, J. A. K. Howard, H. Puschmann, *J. Appl. Cryst.* **2009**, *42*, 339-341.

[36] a) L. Palatinus, G. Chapuis, *J. Appl. Cryst*. **2007**, *40*, 786-790; b) L. Palatinus, A. van der Lee, *J. Appl. Cryst*. **2008**, *41*, 975-984; c) L. Palatinus, S. J. Prathapa, S. van Smaalen, *J. Appl. Cryst.* **2012**, *45*, 575-580.

[37] G. M. Sheldrick, *Acta Cryst*. **2008**, *A64*, 112-122.

…

Entry for the Table of Contents (Please choose one layout)

Layout 1:

FULL PAPER

We have conjugated a photoactivatable Pt^{IV} pro-drug to guanidinoneomycin and studied its photoactivation properties in the presence of 5'-GMP and of a synthetic oligonucleotide. The phototoxicity of the compound towards cancer cell lines in the presence of blue light and cellular uptake by ICP-MS were also investigated.

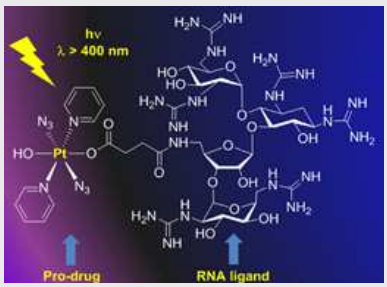

Evyenia Shaili, Marta Fernández-Giménez, Savina Rodríguez-Astor, Albert Gandioso, Lluís Sandín, Carlos García-Vélez, Anna Massaguer, Guy J. Clarkson, Julie A. Woods, Peter J. Sadler, Vicente Marchán**

Page No. – Page No.

A photoactivatable Pt^{IV} anticancer complex conjugated to the RNA ligand guanidinoneomycin

Layout 2:

FULL PAPER

((Insert TOC Graphic here; max. width: 11.5 cm; max. height: 2.5 cm))

*Author(s), Corresponding Author(s)**

Page No. – Page No.

Title

Text for Table of Contents